



HAL
open science

Characterization of a new generation of silicon detector: The SIRIUS side “Strippy-Pad” detector

P. Brionnet, H. Faure, O. Dorvaux, B. Gall, K. Hauschild, C. Mathieu, E.
Gamelin

► To cite this version:

P. Brionnet, H. Faure, O. Dorvaux, B. Gall, K. Hauschild, et al.. Characterization of a new generation of silicon detector: The SIRIUS side “Strippy-Pad” detector. Nuclear Instruments and Methods in Physics Research Section A: Accelerators, Spectrometers, Detectors and Associated Equipment, 2021, 1015, pp.165770. 10.1016/j.nima.2021.165770 . hal-03552830

HAL Id: hal-03552830

<https://hal.science/hal-03552830v1>

Submitted on 16 Oct 2023

HAL is a multi-disciplinary open access archive for the deposit and dissemination of scientific research documents, whether they are published or not. The documents may come from teaching and research institutions in France or abroad, or from public or private research centers.

L'archive ouverte pluridisciplinaire **HAL**, est destinée au dépôt et à la diffusion de documents scientifiques de niveau recherche, publiés ou non, émanant des établissements d'enseignement et de recherche français ou étrangers, des laboratoires publics ou privés.



Distributed under a Creative Commons Attribution - NonCommercial 4.0 International License

Characterization of a New Generation of Silicon Detector: the SIRIUS Side “Strippy-Pad” Detector

P. Brionnet^{a,1}, H. Faure^a, O. Dorvaux^a, B. Gall^a, K. Hauschild^b, C. Mathieu^a, E. Gamelin^a for the SIRIUS-S³ collaboration

^aIPHC-DRS/Université de Strasbourg, IN2P3-CNRS, UMR 7178, F-67037 Strasbourg, France

^bIJCLab, Université Paris-Saclay, IN2P3-CNRS, UMR 9012, F-91405 Orsay, France

Abstract: SIRIUS (Spectroscopy & Identification of Rare Isotopes Using S³) is a detection system designed for the focal plane of S³ (the Super Separator Spectrometer), which is part of the SPIRAL2 (Système de Production d'Ions Radioactifs en Ligne de 2e génération) facility at GANIL (France). This study presents the characterization of the Side silicon detector of SIRIUS. This new “Strippy-pad” detector design benefits from an ultra-high resistivity and the windowless technique from Micron Semiconductor Ltd. These detectors were tested at the IPHC Strasbourg on a dedicated test bench with custom fast preamplifiers coupled to digital electronics cards. Combining all these elements, we obtained resolutions as good as 13.6 keV for certain pixels of this detector for 8.8 MeV alpha particles, with an average resolution measured at 14.7 keV over the whole detector.

Keywords: Tracking and position-sensitive detectors, Solid-state detectors, Double Sided silicon Detectors, Charged-particle spectroscopy, alpha particle detection, Electron spectroscopy

1. INTRODUCTION

One of the main challenges in modern nuclear physics is the study of nuclei far from stability, which provides strong constraints for nuclear models. Closed nucleonic shells are clear fingerprints of quantal behaviour of nuclei leading to the so-called magic numbers of neutrons or protons. The region around the doubly magic ¹⁰⁰Sn and the region of very heavy and super heavy nuclei are excellent nuclear structure physics cases to study these extreme magic systems and for the quest of an ultimate island of stability.

The very low production cross-section of these nuclei needs to be compensated by improving the sensitivity and efficiency of the experimental setups. The present development is performed within the S³ [1] (Super Separator Spectrometer) project, which is a part of the new SPIRAL2 (Système de Production d'Ions Radioactifs en Ligne de 2e génération) facility at GANIL (Caen, France). SIRIUS [1] (Spectroscopy & Identification of Rare Isotopes Using S³) is the detection system designed and optimized for spectroscopic studies of rare exotic isotopes and heavy/super-heavy elements at the final focal plane of S³. Its compact geometry combined with new advanced technologies, such as new detector designs, customized preamplifiers and adapted digital electronics, allows for a large range of energies to be covered (from low-energy electrons, ~50 keV, to heavy fission fragments, ~100-200 MeV) with resolution (from 0.2% for the typical alpha energies and up to 1% for the heavy ions [1]).

Ions enter the SIRIUS focal plane detector array through the large-area tracker detector for time of flight, ion tracking as well as mass measurement. These ions are then implanted into a 10 × 10 cm² Double-sided Silicon Strip Detector (DSSD, also called implantation detector) segmented in 128 strips on each side. Implanted nuclei, as well as alpha particles and conversion electrons emitted by the subsequent decays, are also partially detected in the DSSD. Four large silicon detectors are placed in a “tunnel” configuration, upstream from the DSSD to detect alpha particles and electrons escaping from the DSSD. An array of five Germanium clover detectors for gamma ray spectroscopy is placed as close as possible around this “silicon box” (one behind the DSSD and 4 around the Side detectors in a cross configuration, Fig. 1 [2]). All detected decay events are individually time-stamped in dedicated digital electronics modules.

picture1.jpg

¹ Present address RIKEN Nishina Center for Accelerator-Based Science, Saitama 351-0198 Japan ; pierre.brionnet@riken.jp

1.1 Detector Characteristics and Design

The Side detectors of SIRIUS are part of the new generation of silicon detectors produced by Micron Semiconductor Ltd. These detectors are produced using a high resistivity silicon wafers (20-50 K Ω .cm) made from N-Type silicon with the orientation <100>. With a thickness of ~700 μ m and large active area (10 \times 10 cm²), they have a surface capacitance of 19.71 pF.cm⁻² at full depletion voltage. Finally, due to their dead layer thinner than 50 nm (typically around 30 nm, as provided by Micron Semiconductor Ltd under their 9.5P denomination [3]) are called “windowless”. This new design of “Strippy-Pad” (Fig. 2) detectors is composed of 64 pixels (pads) on the ohmic side and one large single windowless pixel side with 3% grid coverage (for good charge collection) on the junction side.

Picture2.jpg

Each pad has a peripheral metallization (Fig. 3) for charge collection associated with a 30 μ m wide strip connected to a bonding pad. The bonding pads are gathered into four groups (two columns of 8 pixels in each group), and are located on the same edge of the detector (Fig. 2). To avoid charge trapping under the usual insulation layer between the wafer and the metallic collection strip, the signal-tracking were designed as active strips (i.e., metallic deposit on an active volume of silicon Fig. 3, rather than the metallic deposit being insulated from the wafer by an oxide layer). These metallic strips are located between every two columns of pixels. Due to this design, the surface of each pixel, as well as the tracking length, differs from one pixel to the next. Thus, the measured pixel capacitances range from 51 pF (large pixels area and long tracking: 1.4484 cm² and 8.51 cm of tracking) down to 32 pF (smaller active area: 1.356 cm² and no tracking next to the bounding pads).

Picture3.jpg

This “Strippy-Pad” concept [4,5] enables windowless operating for a pad detector by avoiding the dead layer associated with the double metal technique usually used for pads, as well as the insulation oxide layer for the metallic strip. This design also allows the connectors to be located only on one side, on the “bottom”-side of the detector frame, to ensure a very compact geometry of SIRIUS.

An innovative hybrid support frame, combining an anodized aluminium frame for an efficient cooling and a PCB for the connectors and signal transmission, were developed at the IPHC Strasbourg (Fig. 2). Good cooling and grounding properties of this detector are provided by the aluminium frame. In addition to the opening dedicated to the silicon detector wafer, and to minimize the absorption of low-energy gamma- and X-rays, a shallow volume is machined at the bottom of the aluminium frames for the positioning of a double-sided PCB board. This board bridges the signals from the detector to the output cables. Bonding pads are placed facing the detector field plate, guard rings and pixel bonding pads. Connection to the preamplifier is made via two 40-channel compact cables onto SAMTEC connectors. The PCB board is glued onto a non-anodized recess into the aluminium frame using a silver-loaded glue to ensure good grounding connection. This hybrid frame allows for a compact mounting of the five detectors (Four Side detectors and one implantation detector) into a silicon-box geometry.

1.2 SIRIUS Detectors Test Bench

The characterization of the Side detectors of SIRIUS was performed at the IPHC Strasbourg using a dedicated test bench [[6], page 151-155]. It is composed of a chamber for operation under controlled vacuum/temperature and a digital acquisition chain based on TNT2 cards [7]. A copper cooling plate was designed to be able to either place the ohmic (or the junction) side in front of a radioactive source inside the vacuum chamber. Four radioactive sources were available (²⁰⁷Bi, ¹³³Ba, ²¹²Pb and a mixed ²³⁹Pu/²⁴¹Am/²⁴⁴Cm) and could precisely be positioned using a SMARACT piezoelectric XY- Θ table combined with a set of collimators.

The acquisition chain is composed of custom CR110 CREMAT preamplifiers [8] combined with digital electronics composed of TNT2 cards [7]. The custom gain of these custom preamplifiers is 173 mV/MeV (rather than 62mV/MeV, both corresponding to unloaded gain) was chosen to get a 14.5 MeV full-scale energy range (i.e. 1.25 Vpp signal) while retaining their very fast response time. For pixels with capacitances in the 30-50 pF range, the response-time of the custom CR110 is 13.2-16.6 ns (0.17 \times C_d (pF) + 3 ns as given by the CREMAT specification sheet [8], where C_d is accounting for detector and cables capacitance (30 pF)) which is much faster than the ~100-150 ns needed for charge collection our silicon and could enable to probe the discrimination between alpha particle and electron through their different collection time. A dedicated 26 channel PCB motherboard was developed at the IPHC to host these preamplifiers. After the pre-amplification stage, the signals are

98 digitized at a sampling rate of 100 MHz rate using 7 TNT2 cards [7] developed at IPHC Strasbourg. These 4 channels TNT2
99 boards are based on 14-bit flash ADC's operating at 100 MHz. Each channel is treated independently and in parallel. Moreover,
100 they can generate online spectra as well as to store individual oscillograms (traces) to disc for offline treatment. The energy
101 measurement is performed using trapezoidal shaping provided by a Jordanov algorithm [9] implemented on the FPGA of the
102 TNT2 board. After setting the proper pole zero correction for each individual channel, this pipe-line data processing of the
103 energy is defined by 2 parameters: integration time, and flat top duration of the trapezoid (defined for each channel
104 individually).

105 2. VALIDATION OF THE DETECTORS

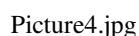
106
107 This paper is focused on the validation of the concept of the "Strippy-Pad" detector. Two detectors were characterized during
108 this work. The results presented here report on the first one, the characteristic of the second one being very similar.

109 2.1 Reduced Number of Channels by Pixel Grouping

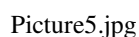
110 Even though the "Strippy-Pad" detector was designed and produced with 64 pixels, it was foreseen from the beginning to
111 reduce this number by making macro-pixels. Indeed, in order to meet the specifications of the SIRIUS collaboration, the number
112 of channels per detector needed to be reduced, with the condition that the maximum energy resolution should remain below 20
113 keV for 8 MeV alpha particles. A good pixel granularity near the DSSD is required to limit the dead layer effect on the escaped
114 alpha particles [Courtesy of A. Lopez-Martens, [5]], and lower granularity can be accepted further away from the DSSD. It is
115 worth pointing out that these constraints lead to the grouping of lower capacitance pixels rather than higher capacitance ones.

116 We established that the capacitance of the macropixels should remain under 145 pF in order to minimize the influence of the
117 capacitance noise from the CREMAT preamplifier on the measured resolution (less than 10% of the 20 keV of the
118 specification); considering the equivalent noise charge slope (3.8 e⁻RMS/pF) and the average energy for a pair creation in the
119 silicon (3.62 eV). Moreover, the intrinsic noise of the system at 0 pF was less than 5 keV (1.7 keV coming from the preamplifier
120 [8])

121 Several possible schemes of macropixels structures corresponding to 16, 20 or 24 groups were studied. Since the structure of
122 the "Strippy-Pad" presents four identical blocks composed of 2 columns of 8 pixels with their respective strips, the reduced
123 schemes were designed around this elementary block. Several reduced configurations were selected by the collaboration and
124 fully characterized. However, two were selected, based on their performances and have been used for the present work. Fig. 4
125 illustrates both the mapping of the macropixels used during this work (Fig. 4 (a)) and the two macropixels configurations
126 selected (Fig. 4 (b)). The final choice between these two configurations was left to the collaboration.

127
128
129 

130
131 Practically, the number of pixels is reduced physically by using a PCB board plugged between the connector and the Kapton
132 cable (Fig. 5) grouping the pixels into the macropixels.

133
134
135 

136 2.2 Testing Protocol

137 A two-step protocol was established to test the detectors upon delivery and to precisely determine the optimal operating
138 conditions for each detector. This protocol will be applied for the validation tests of every Side detector that the collaboration
139 order.

141 2.2.1 Depletion Voltage and Operating Voltage Determination

142
143 After a visual inspection under binocular lenses, the detector is characterized in a clean room. During this step, done in a
144 dark room, one measures pixel by pixel the current (Keithley 6487 (set V and read I) Fig. 6.b) and capacitance (Keithley 6487
145 (set V) and Boonton 7200 (read C) Fig. 6.a) evolution with applied voltage. This characterization enables us to determine the
146 full depletion voltage of the detector (VD), the possible operating voltage range as well as the good behaviour of every single
147 pixel (not macropixel).
148

149
150 Picture6.jpg

151
152 For this particular detector, the full depletion voltage (VD) is at 50 V from the capacitance plots (Fig. 6 (a)); Above VD,
153 there are no more changes in the measured capacitances, capacitance stabilizes around a constant value. This value is consistent
154 with the value given by Micron Semiconductor Ltd. as well as the value obtained from the current versus voltage plot (start of
155 the plateau observed in Fig. 6 (b)). Thus, the range of operation of the detector was chosen to be above 1.5xVD and below 150V
156 (according to the recommendation of MICRON Semiconductor Ltd.).
157

158 2.2.2 Optimal Working Point

159
160 In a second step, we tune the applied voltage and the detector operating temperature by monitoring the energy resolution of
161 detected alpha particles. A resolution versus temperature and voltage matrix is first constructed with data from the TNT2 energy
162 spectra using the trapezoidal rising time and flat top duration known to give good resolution from previous detectors; The pole
163 zero compensation was optimized channel by channel once and for all at the beginning of the characterization.

164 The Fig. 7 illustrates such evolution of the measured energy resolution (all energy resolutions in this article will be given in
165 FWHM). For this detector, the best resolution is obtained at 80V and -20 °C. However, this graph does not show the error bars
166 on the measured resolution: typically below 0.5 keV on the FWHM. Thus, once the applied voltage and temperature reach the
167 plateau (above 80 V and below -5 °C), every point is expected to behave the same regarding the measured resolution within the
168 error bars. However, the evolution of the energy resolution is quite sensitive to change of both voltage and temperature at the
169 edges of this operating region. Therefore, a slightly higher applied voltage was preferred and enabled higher operating
170 temperature. The working point was then set at 90 V and -15 °C for this detector.
171

172
173 Picture7.jpg

174
175 Once this working point is determined, we accumulated a significant number of preamplifier signal traces (~10000 per alpha
176 line) in order to get a statistical data set for the full detector. An offline analysis code processed the recorded signal traces and
177 was used to optimize the Jordanov [9] parameters to obtain the best energy resolution using a 100 ns increments. Fig. 8 shows
178 the resolution for the 8.8 MeV ^{212}Po alpha line as a function of the trapezoidal integration time and flat top duration. The best
179 resolution is obtained for a quasi-triangular configuration: 4.8 μs integration time and 350-400 ns of flat top duration for this
180 particular macropixel.
181

182
183
184 Picture8.jpg

185
186 For flat top durations of 0 to 200 ns (cf. Fig. 8, corresponding to quasi-triangular shape) a drastic increase in the measured
187 FWHM was observed as expected. This width corresponds to the signal rise time of ~100-150 ns. This effect has already been
188 observed and discussed in [10]. Fig. 8 corresponds to a typical macropixel within the average resolution measured. Such an
189 optimization has been performed for each macropixel within the same run, since our data file contains traces from the full
190 detector. This allows us to determine the optimal parameters over the whole detector. According to this measurement, the
191 optimal working point is for a rise time of 5 μs and a flat top time of 0.4 μs for this particular detector.
192

193 2.3 Macropixel Resolution

194
195 Macropixels were characterized with a mixed $^{212}\text{Po}/^{212}\text{Bi}/^{212}\text{Po}$ alpha emitting source obtained from the deposition of ^{216}Po
196 onto a gold foil during the decay of the ^{232}Th through the gaseous alpha decay of the ^{220}Rn to avoid any source thickness effect
197 on the alpha energy. A typical ^{212}Pb alpha spectrum can be seen in Fig. 9 with very good resolution within the whole alpha
198 energy range. This spectrum was obtained at (90V, -15 °C) following the optimization of the Jordanov parameters, with an
199 energy resolution of 13.66 keV for the 8.783 MeV ^{212}Po line. The fitting function used during this work is the derived from the
200 SAMPO gamma-ray program, which is a modified Gaussian distribution [11].
201
202

203 Picture9.jpg

204

205 Resolutions are reported in Fig. 10 as a function of the capacitance of the macropixel for the two selected reduced pixel
206 configurations. The average value of energy resolutions obtained is about 14.7 keV over the full detector for the ^{212}Po 8.783
207 MeV alpha line. This figure shows a slight increase in the measured average FWHM with capacitance of about 0.6-0.7 keV on
208 average from the low capacitance macropixel to the high capacitance ones (from 14.4 keV to 15-15.1 keV). The expected
209 contribution of the intrinsic noise of the preamplifier is 3.8 e-(RMS)/pF, thus leading to a 3.1 keV contribution to the FWHM at
210 95 pF and 4.7 keV at 146 pF. Moreover, the noise contributions add in quadrature. Thus, if we take the 14.4 keV FWHM at 95
211 pF, the "intrinsic" FWHM will be 14.1 keV leading to a 14.9 keV at 146 pF just based on the contribution from the preamplifier
212 which is in good agreement with the measurements.

213 In addition, all the FWHM values measured during these characterizations are within the specifications of the project, with
214 every single macropixel below the 20 keV upper limit.

215

216 Picture10.jpg

217

218 2.4 Determination of the Diode Orientation

219

220 The tunnel detectors collect electrons from internal conversion electrons (ICE) as well as escaping alpha particles from decays
221 occurring within DSSD detector. The energy range of these particles is in principle significantly different, enabling a selection
222 with a single energy deposit threshold. Unfortunately, due to the energy deposition in the DSSD while escaping and the dead
223 layer effect in the Side detector, the residual energy from alpha particles can be pushed down to the energy range of ICE. This
224 overlapping is particularly damaging for energies below 300 keV. Fortunately, the range of both particles in silicon differs, thus
225 inducing noticeable difference in collection timings even with similar number of charges to be collected. The main key points in
226 the discrimination between the electron signals and escaped alpha signals when they have similar amplitude in a Side detector
227 (100-300 keV energy range) is the optimization of the physical characteristic of the pulse shape of the signal. In that sense, a
228 correct choice of the orientation of the silicon detector with respect to the alpha emission (decay of implanted heavy ions in
229 DSSD) is mandatory.

230 In order to investigate this point, our Strippy-pad detectors were designed with zero dead layer on both junction and ohmic
231 sides. Fig. 11 illustrates in that sense the difference of pulse shapes observed for detection of alpha particles on the ohmic side
232 (blue) and on the junction side (red). A difference of rise-time of about 50 ns is observed, as expected. This is due to the
233 difference in mobility of the charge carrier inside the silicon, as well as the very small range of alpha particles in silicon.

234

235

236 Picture11.jpg

237

238 As alpha particles are being stopped in the first few micrometers of the detector, the charge collection time will mainly be
239 driven by one charge carrier, the opposite one being created very close to its collecting electrode. Therefore, only one type of
240 charge carrier will drive the rise-time of the signal. Indeed, in the case of the junction-side detection the signal rise-time is
241 shorter, as the signal will be mainly driven by the electron, compared to the ohmic implantation where the signal is due to the
242 motion of holes through the entire thickness of the detector (Fig. 11).

243 We can confirm the difference in rise-time for the alpha particles: as predicted, the one on the ohmic side is slower. Indeed,
244 the electrons have a deeper implantation depth in the silicon (~50 μm to a few hundreds of micrometers depending on their
245 energy) than the alpha particle (few micrometers only). Thus, by using the slower signal for the alpha particle, we should have a
246 better chance to discriminate between the two signals in the low-energy range (100-300 keV). This observation in the difference
247 in mobility for holes and electrons inside silicon firmly points out the orientation of our detector inside the silicon box.

248 Moreover, the fastest collection time in the detector is not at the surface of the junction side where the holes are collected
249 immediately, but slightly deeper. In our case (90 V and -10 °C), the fastest collection is about 120 μm from the Junction side,
250 where electrons and holes have the same collection time. Thus, if the junction side was selected to face the DSSD, the difference
251 between alpha and electron signal of low energy would have been less than 5 ns. But, in the case of the ohmic side, this
252 difference should be around 10-20 ns due to the slow collection time of the holes.

253 The optimal orientation was determined by setting the inner face inside our 3D assembly to the ohmic side, which that should
254 give the best potential discrimination properties (slower signal) between alpha particles and electrons. This decision triggered

255 the development of the hybrid frame for the final assembly (Fig. 1.); the design of the frame and double-sided PCB depended on
256 the choice of orientation.

257 **CONCLUSION:**

258
259 Two new generation silicon detectors for the S3-SIRIUS focal plane Side detectors were characterized during this work. These
260 detectors have 64 pixels on the ohmic side and a wide pixel on the junction side. A macropixel grouping of the 64 individual
261 pixels was used to determine two 24-channel configurations for the collaboration, while maintaining the possibility to operate in
262 single pixel mode in the future. Very good alpha energy resolution was achieved with overall resolutions (FWHM) better than
263 18 keV for 8.8 MeV alpha line and the best macropixels as low as 14.8 keV. These innovative detectors largely meet the
264 SIRIUS collaboration specifications. They will be used for the physics program of S3.

265 **ACKNOWLEDGMENT**

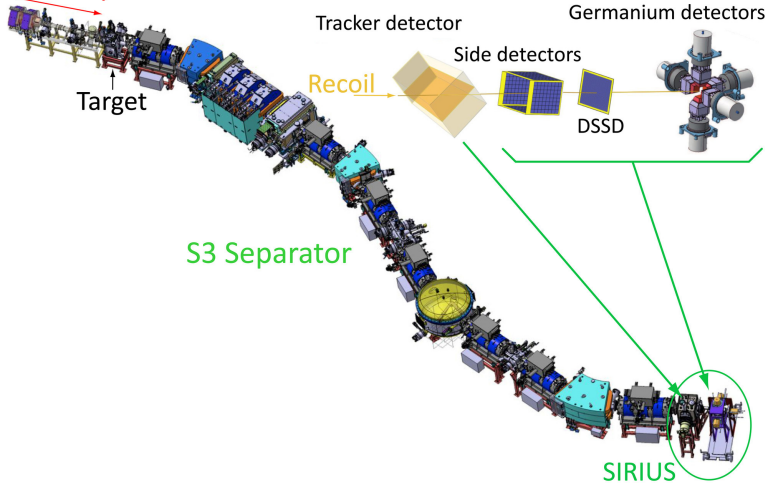
266 The authors warmly thank the mechanical service of the IPHC Strasbourg for their work and support on the test bench
267 development, on the hybrid frame design as well as the 3D mounting system of SIRIUS. We would like to address special
268 thanks to M. Richer for the support on TNT2 operation, to the IPHC microtechnics services as well as to N. Karkour for their
269 support and last but not least the present and former members of the S3-SIRIUS collaboration. The authors would like to
270 express their gratitude to Micron Semiconductor Ltd for their expertise that enabled the realization of this project and to F.
271 Olschner from CREMAT Inc. for the developments of our customs preamplifiers.

272 **REFERENCES**

- 273 [1] F. Dechery et al., "Toward the drip lines and the superheavy island of stability with the Super Separator Spectrometer S3."
274 Eur. Phys. J. A (2015) 51- 66
- 275 [2] J. Piot for the S3 Collaboration, "Studying Nuclear Structure at the extremes with S3", EPJ Web of Conference 178 (2018),
276 <https://doi.org/10.1051/epjconf/201817802027>
- 277 [3] MICRON Catalogue [http://www.micronsemiconductor.co.uk/wp-content/uploads/2018/03/2018-Micron-Semiconductor-](http://www.micronsemiconductor.co.uk/wp-content/uploads/2018/03/2018-Micron-Semiconductor-Ltd-silicon-Catalogue_Long-Form.pdf)
278 [Ltd-silicon-Catalogue_Long-Form.pdf](http://www.micronsemiconductor.co.uk/wp-content/uploads/2018/03/2018-Micron-Semiconductor-Ltd-silicon-Catalogue_Long-Form.pdf) (last open 29/03/2021)
- 279 [4] H. Faure, Proc. Conf. on Advancements in Nuclear Instrumentation, Measurement Methods and Their Applications,
280 ANIMMA 2013, <http://dx.doi.org/10.1109/ANIMMA.2013.672808>
- 281 [5] B. Gall et al., ActaPhys. Pol. B Vol 42 (2011) 597-604
- 282 [6] P. Brionnet, PhD Thesis, University of Strasbourg N°3844, 2017
- 283 [7] L. Arnold et al., "TNT digital pulse processor". IEEE Transactions on Nuclear Science, 53(3) : 723, June 2006.
- 284 [8] Technical description at <https://www.fastcomtec.com/fwww/datashee/amp/cr-110.pdf> (last open 29/03/2021)
- 285 [9] Valentin T. Jordanov, Glenn F. Knoll, Alan C. Huber, John A. Pantazis, "Digital techniques for real-time pulse shaping in
286 radiation measurements", NIMA A 353 (1994) 261-264
- 287 [10] Valentin T. Jordanov, Glenn F. Knoll, "Digital synthesis of pulse shapes in real time for high-resolution radiation
288 spectroscopy", NIMA A 345 (1994) 337-345
- 289 [11] C. John Bland, "Choosing fitting function to describe peak tails in Alpha-particle Spectrometry", App. Radiat. Isot. Vol. 49,
290 No 9-11, pp. 1228-1229, 1998

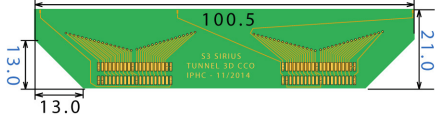
291

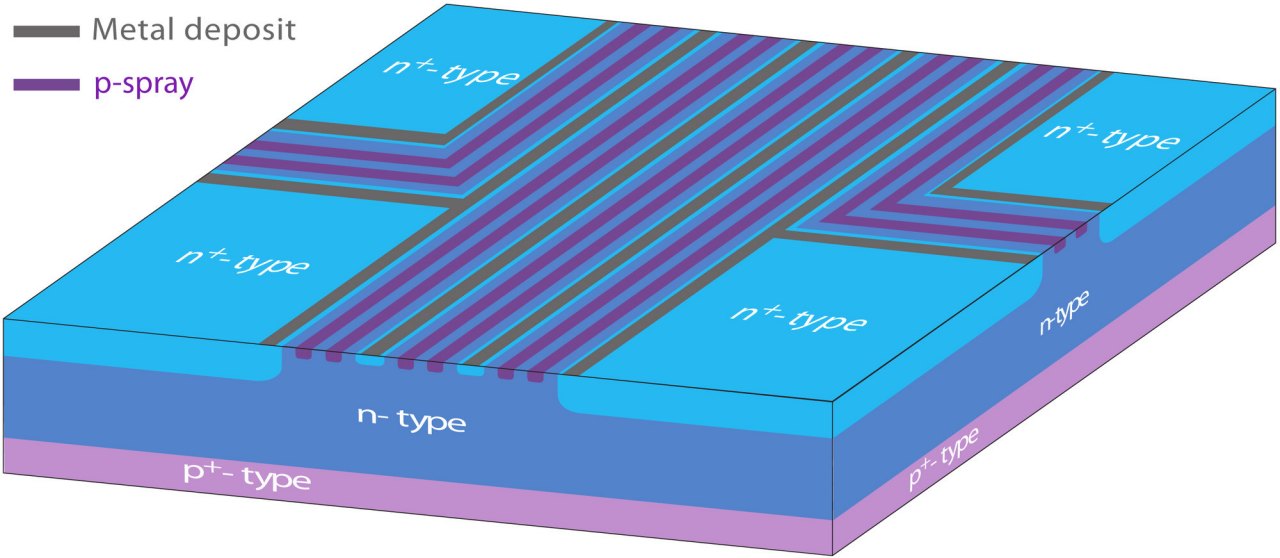
Primary Beam

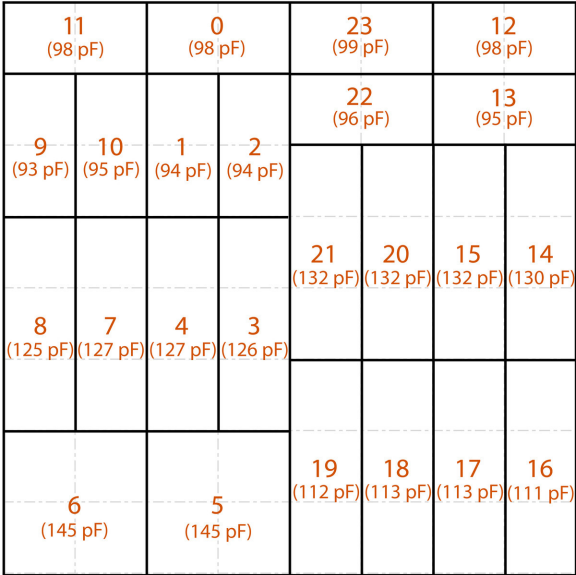


S3 Tunnel detector
100.42 X 100.42 mm²
670 μm thick
Ohmic side
(Back)

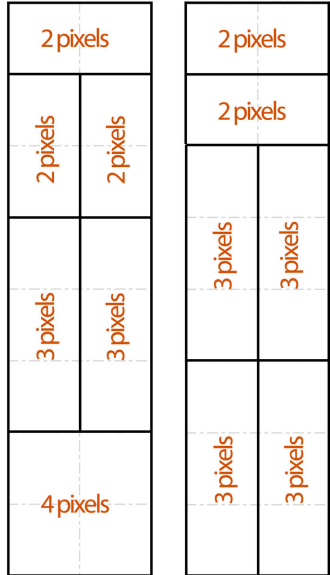
S3 Tunnel detector
100.42 X 100.42 mm²
670 μm thick
Junction side
(Front)







(a)



(b)

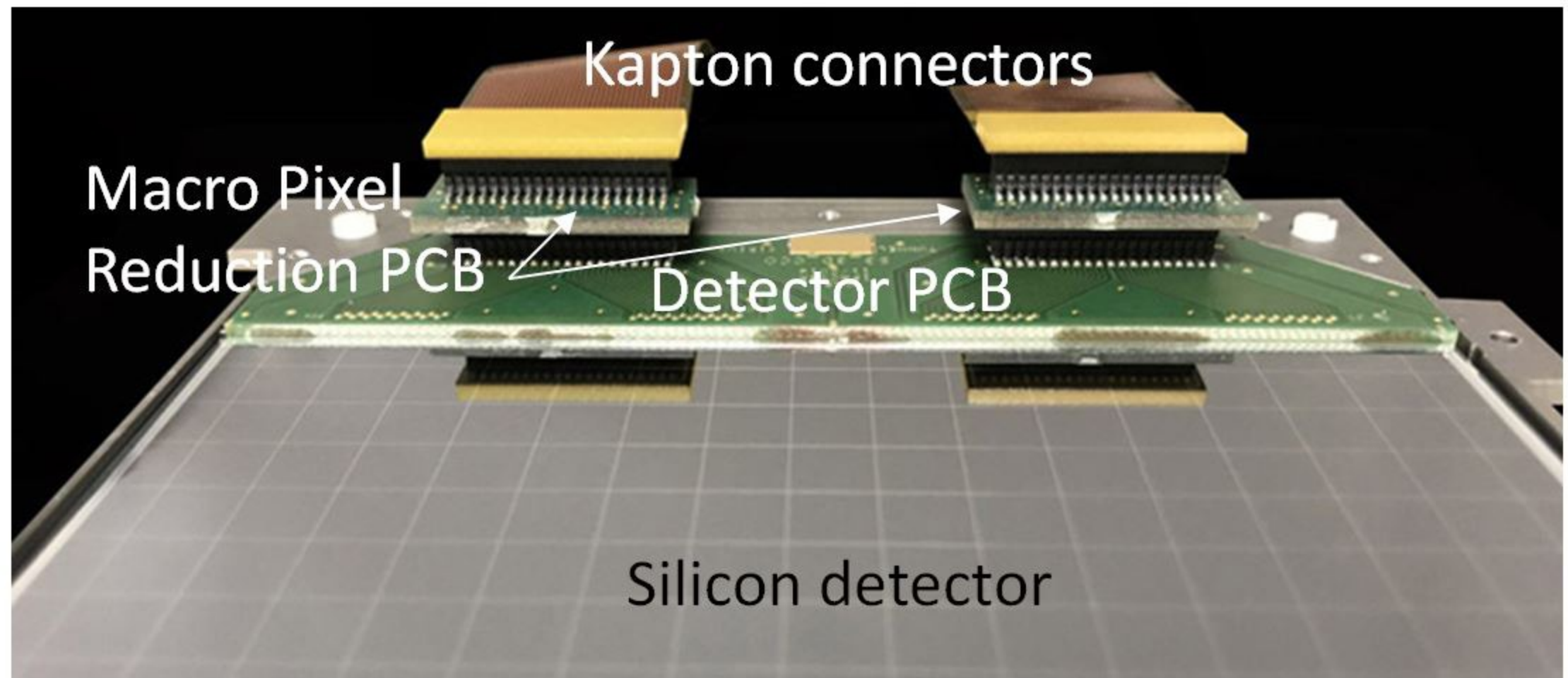
Kapton connectors

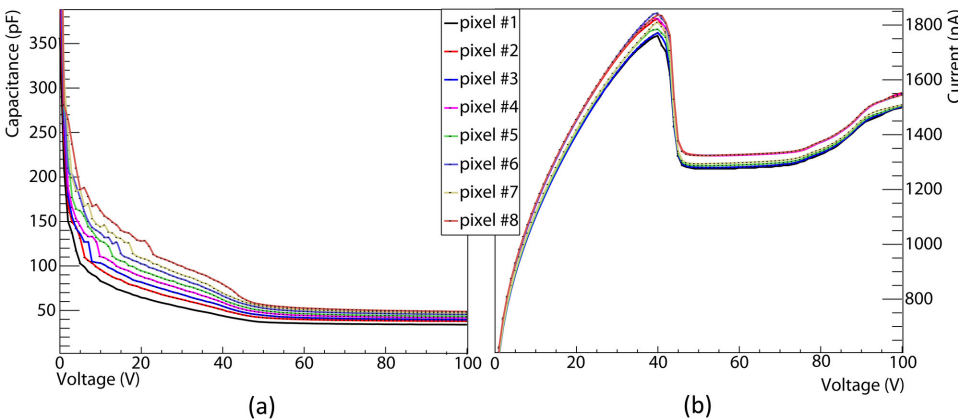
Macro Pixel

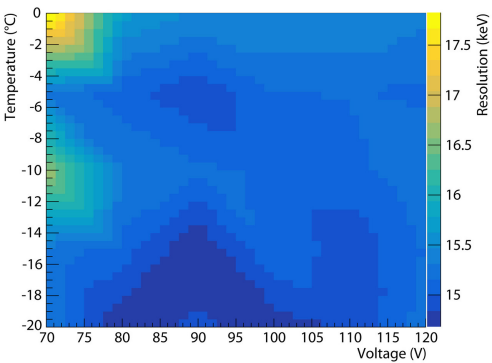
Reduction PCB

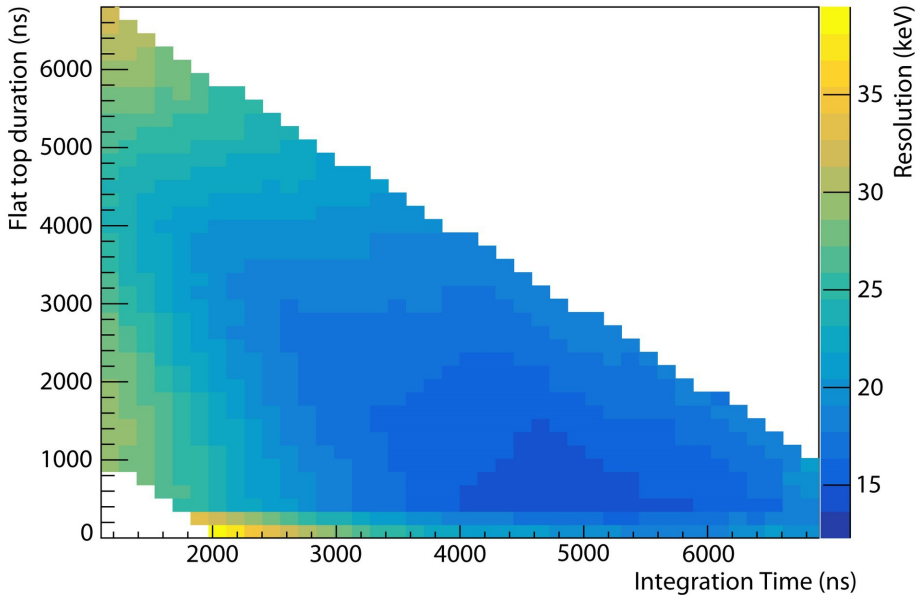
Detector PCB

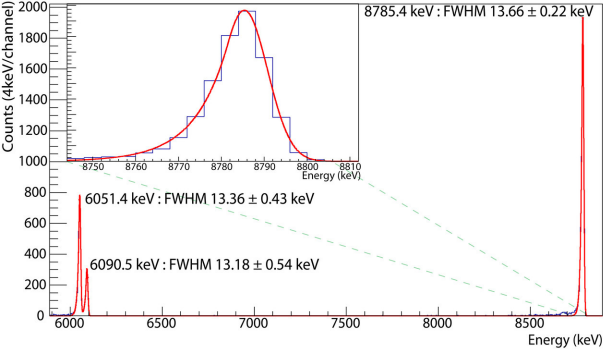
Silicon detector



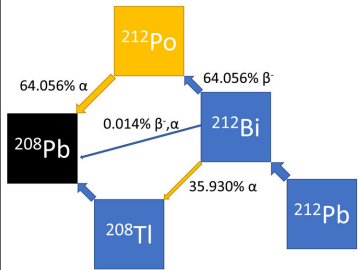








a)



b)

